ISWI is a RanGTP-dependent MAP required for chromosome segregation

Hideki Yokoyama, Sofia Rybina, Rachel Santarella-Mellwig, Iain W. Mattaj, and Eric Karsenti

European Molecular Biology Laboratory, Heidelberg 69117, Germany

Production of RanGTP around chromosomes induces spindle assembly by activating nuclear localization signal (NLS)–containing factors. Here, we show that the NLS protein ISWI, a known chromatin-remodeling ATPase, is a RanGTP-dependent microtubule (MT)-associated protein. Recombinant ISWI induces MT nucleation, stabilization, and bundling in vitro. In *Xenopus* culture cells and egg extract, ISWI localizes within the nucleus in interphase and on spindles during mitosis. Depletion of ISWI in egg extracts does not affect spindle assembly, but in anaphase spindle MTs disappear and chromosomes do not segregate. We show directly that ISWI is required for the RanGTP-dependent stabilization of MTs during anaphase independently of its effect on chromosomes. ISWI depletion in *Drosophila* S2 cells induces defects in spindle MTs and chromosome segregation in anaphase, and the cells eventually stop growing. Our results demonstrate that distinctly from its role in spindle assembly, RanGTP maintains spindle MTs in anaphase through the local activation of ISWI and that this is essential for proper chromosome segregation.

Introduction

In addition to their function as data storage devices, chromosomes have more recently been shown to play an important organizational role in the cell. In interphase they organize the nucleo-cytoplasmic transport, and during mitosis they drive spindle assembly in metaphase and nuclear envelope and nuclear pore complex assembly in telophase (Clarke and Zhang, 2008). In each case, the guanine nucleotide exchange factor for Ran (RCC1) is bound to chromosomes and the Ran-GTPase activating protein (RanGAP) is distributed throughout the cytoplasm. As a consequence, the GTP bound form of Ran (RanGTP) is locally produced inside the nucleus in interphase and in a gradient surrounding the chromosomes during mitosis (Hetzer et al., 2002). The RanGTP gradient induces spindle assembly through the local activation of several NLS-containing molecules (Kalab and Heald, 2008), examples being the microtubule (MT) nucleator TPX2 and the MT stabilization factor CDK11 (Gruss et al., 2001; Yokoyama et al., 2008). Both TPX2 and CDK11 are inhibited by the importin-α/β heterodimer in the mitotic cytoplasm and released from it when RanGTP binds to importin-β around chromosomes. Because all NLS proteins are released from importins locally around chromosomes in mitosis, they are potentially involved in spindle assembly or other chromosome-dependent processes. We have recently established an affinity purification method to isolate pure NLS proteins from *Xenopus* egg extracts, by optimizing the elution of NLS proteins from importin-β affinity column (Yokoyama et al., 2008). We are in the process of characterizing the functions of components in the NLS fraction.

Here, we report on one of these NLS proteins, ISWI, initially characterized as a chromatin-remodeling ATPase (Brown et al., 2007). We find that ISWI is a RanGTP-dependent microtubule-associated protein (MAP) in vitro. This protein is not required for spindle assembly, but is essential for chromosome segregation. This anaphase function involves a RanGTP-dependent stabilization of spindle MTs.

Results

ISWI is a RanGTP-dependent microtubule-binding protein

Previously, NLS-containing MAPs had been prepared by sequential purification of MAPs and importin-β–binding proteins,

Correspondence to Hideki Yokoyama: yokoyama@embl.de; or Eric Karsenti: karsenti@embl.de.

Abbreviations used in this paper: CSF, cytostatic factor; MAP, microtubule-associated protein; MT, microtubule.

The Rockefeller University Press $30.00
J. Cell Biol. Vol. 187 No. 6 813–829
www.jcb.org/cgi/doi/10.1083/jcb.200906020

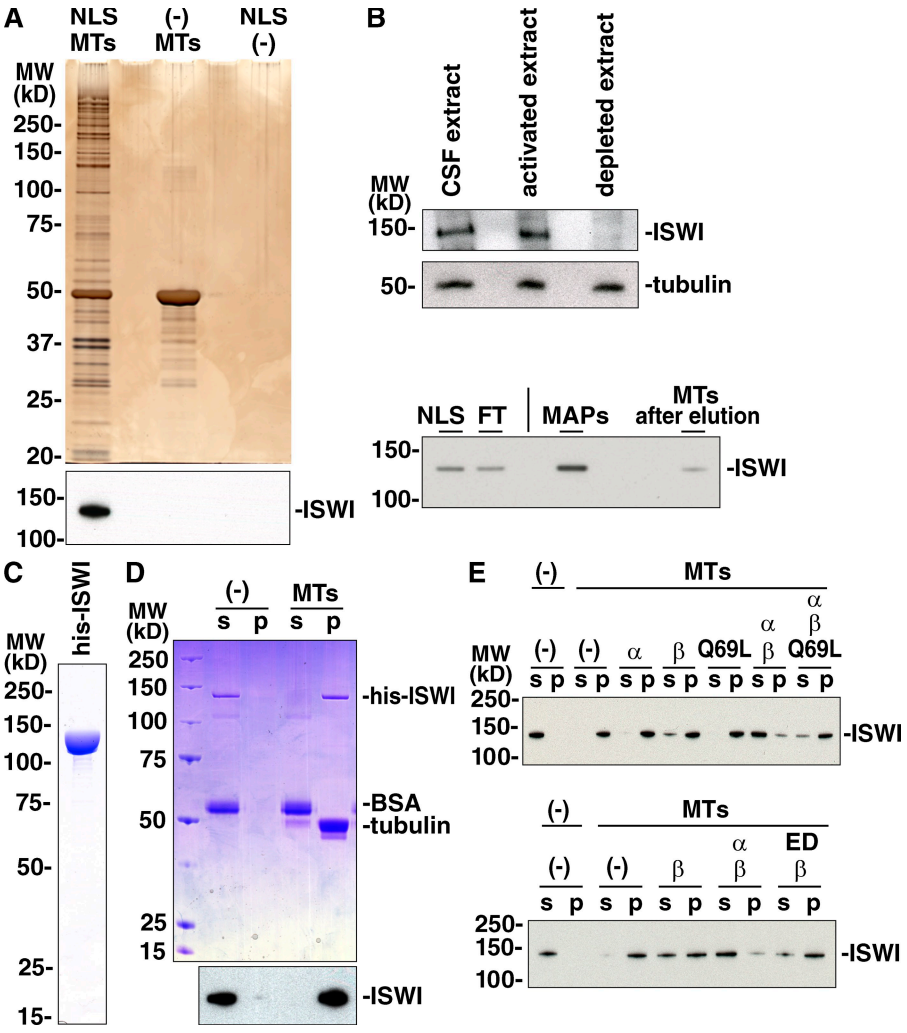

Figure 1. **ISWI is a novel RanGTP-dependent MAP bearing NLS.** (A) Preparation of MAPs from the NLS protein fraction and identification of ISWI in the MAP fraction. The NLS protein fraction (NLS) was incubated with taxol-stabilized pure MTs. The MTs were sedimented and MAPs were eluted with 500 mM KCl. The eluate was resolved on SDS-PAGE for silver staining (top) or immunoblotting with anti-hSNF2H antibody (bottom). (B) Behavior of ISWI during sequential preparation of NLS proteins and MAPs. (Top) To isolate NLS proteins, a CSF extract was treated with RanQ69L beads, the supernatant (activated extract) was further incubated with importin-β beads, and the subsequent supernatant (depleted extract) was recovered. Each extract was blotted with anti-hSNF2H antibody. Tubulin was used as a loading control. (Bottom) To isolate MAPs, the NLS protein fraction (NLS) was incubated with taxol-stabilized MTs and then centrifuged to separate the flow-through (FT) and the MT pellet. The pellet was incubated with 500 mM NaCl and centrifuged again. The supernatant is a fraction containing MAPs and the pellet is the MTs after elution. Each fraction was immunoblotted for ISWI. (C) Recombinant ISWI expressed in insect cells and purified on Talon beads and a Mono S column. Coomassie-stained gel. (D) ISWI directly binds MTs in vitro. Recombinant ISWI (0.25 μM) was incubated with or without taxol-stabilized pure MTs (1 μM) in BRB80 buffer. After centrifugation, supernatant (s) and pellet (p) were resolved on SDS-PAGE for Coomassie staining (top) or immunoblot (bottom). BSA was used as a carrier protein and a negative control that does not bind MTs. (E) Regulation of ISWI binding to MTs by RanGTP and importin-α/β. Recombinant ISWI (0.25 μM) was incubated with 2 μM taxol-stabilized MTs in CSF-XB buffer in the presence or absence of 1 μM importin-α, 1 μM ED mutant, 1 μM importin-β, and 5 μM RanQ69L. After centrifugation, the supernatant (s) and pellet (p) were analyzed by immunoblot using anti-hSNF2H antibody.

resulting in the identification of an NLS-MAP, Xnf7 (Maresca et al., 2005). Following this approach, the NLS fraction prepared from egg extracts (Yokoyama et al., 2008) was incubated with taxol-stabilized MTs and the bound proteins were eluted with high salt (Fig. 1 A). Only a very small proportion of the total NLS proteins bound to the MTs. Nevertheless, the bound fraction that was eluted by high salt still contained a considerable number of proteins (Fig. 1 A). Because ISWI is a nuclear protein that had been reported to bind MTs (Trachtulcová et al., 2000; Liska et al., 2004), we blotted the NLS-MAP fraction with a commercially available anti–human SNF2H antibody (a human orthologue of *Xenopus* ISWI), and indeed we found ISWI in the MAP fraction (Fig. 1 A). We further checked the behavior of ISWI throughout the fractionation of NLS proteins and MAPs (Fig. 1 B). ISWI was depleted from extracts with importin-β beads and efficiently eluted from MTs with high salt, indicating that ISWI is an NLS protein and a MAP.

We then prepared recombinant *Xenopus* ISWI (Fig. 1 C) and examined its ability to bind MTs in a sedimentation assay. Purified ISWI clearly bound to taxol-stabilized MTs (Fig. 1 D). To determine the binding affinity of ISWI for MTs, ISWI (0.50 μM) was sedimented with increasing concentrations of MTs (Fig. S1 A). All of the ISWI was bound to MTs when the MT/ISWI molar ratio was higher than 4. The dissociation constant (Kd) of ISWI at 0.50 μM was calculated to be ∼0.28 μM (the tubulin concentration required to bind 50% of ISWI; Fig. S1 B), indicating that the affinity is relatively high. In addition, ISWI bound to MTs at 1:1 molar ratio under ISWI saturation (Fig. S1 A). This binding was analyzed by electron microscopy showing that ISWI decorates the outer surface of MTs apparently in an organized way (Fig. S1 C).

We then examined whether the MT binding of ISWI was regulated by RanGTP and importins. Addition of importin-β weakly inhibited the binding of ISWI to MTs, whereas importin-α did not (Fig. 1 E). The importin-α/β heterodimer, however, had a significant inhibitory effect on the binding of ISWI to MTs that was reversed by RanQ69L (a mutant of Ran that cannot hydrolyze GTP; Fig. 1 E). Moreover, when we used an ED mutant of importin-α that cannot bind NLS sequences (Gruss et al., 2001), the importin-β/ED heterodimer did not

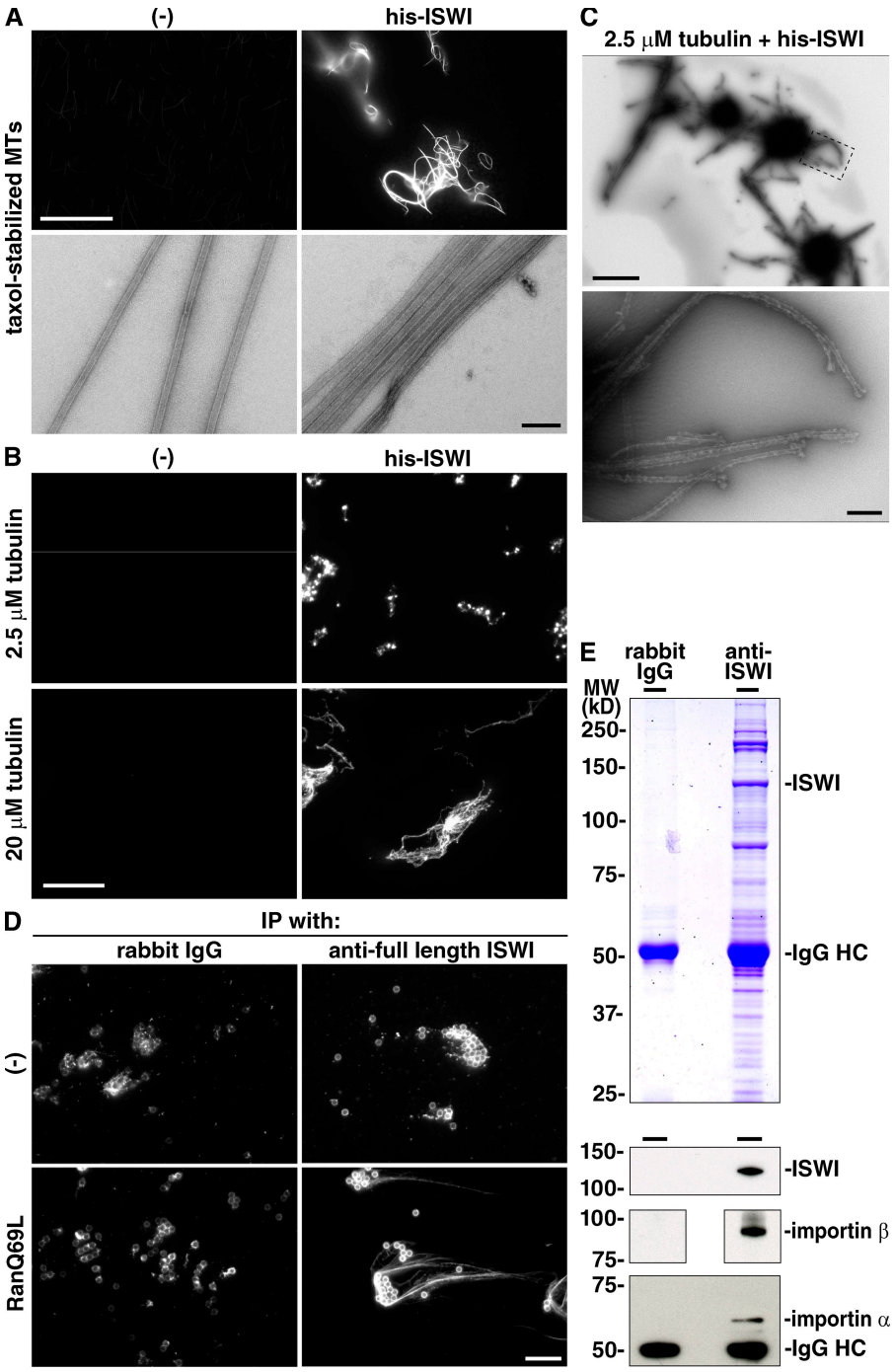

Figure 2. **ISWI assembles MTs in vitro, in a RanGTP-dependent manner.** (A) ISWI bundles MTs in vitro. Recombinant ISWI (1.3 μM) was incubated with 0.3 μM taxol-stabilized MTs incorporating Cy3-labeled tubulin at RT for 20 min. (Top) The samples were squashed without fix solution and immediately imaged. Bar, 20 μm. Note that there are many single MTs in the absence of ISWI. (Bottom) The samples were stained with uranyl acetate and imaged by electron microscopy. Bar, 0.2 μm. (B) ISWI polymerizes MTs and forms asters in vitro. ISWI (2.0 μM) was incubated with 2.5 μM or 20 μM pure tubulin (10% Cy3-tubulin) at 37°C for 30 min. The samples were fixed, spun onto coverslips, and imaged. Bar, 20 μm. (C) EM analysis of the structures assembled in B with 2.5 μM tubulin and 2 μM ISWI. (Top) Low magnification image, showing MT asters. Bar, 2 μm. (Bottom) High magnification image of the dashed box in the top panel, showing plus-end MTs of the aster. Bar, 0.2 μm. (D) RanGTP activates ISWI to polymerize MTs. A CSF extract was incubated with rabbit IgG or anti–full-length ISWI-coated beads. The immunoprecipitates were incubated with 20 μM pure tubulin (2 μM Cy3-tubulin) in the presence or absence of RanQ69L at 37°C for 30 min. The samples were fixed, spun down onto coverslips, and imaged. Bar, 20 μm. (E) ISWI interacts with importin-α and -β. Control and ISWI immunoprecipitates were resolved by SDS-PAGE. (Top) Coomassie staining. (Bottom) Immunoblot with antibodies against ISWI, importin-β, or importin-α.

inhibit the MT binding (Fig. 1 E). This demonstrates that importin-α/β binds to ISWI via an NLS and that this binding inhibits ISWI–MT interaction.

ISWI assembles microtubules in vitro in a RanGTP-dependent manner

The identification of ISWI as a MAP suggested that it might bundle MTs. Indeed, recombinant ISWI strongly bundled taxol-stabilized MTs (Fig. 2 A).

Moreover, recombinant ISWI triggered microtubule assembly when incubated with pure tubulin. At 2.5 μM tubulin, ISWI induced the formation of MT aggregates containing many short MTs (Fig. 2 B). Electron microscopy confirmed that those structures are composed of a number of aster-like structures of MTs (Fig. 2 C). At higher tubulin concentrations (20 μM), ISWI induced the assembly of longer MTs that also frequently formed aster-like structures (Fig. 2 B).

We therefore examined whether ISWI could nucleate MTs. Incubation of GFP-ISWI alone produced some ISWI aggregates (dots; Fig. S2, A–C). In the presence of 2.5 μM tubulin, however, the number of dots increased ∼10 times and they formed MT asters (Fig. S2, B and C). GFP-ISWI and Cy3-tubulin showed the same localization on the dots and MTs. Furthermore, recombinant ISWI-coated beads induced MT growth in

pure tubulin solutions, proving that ISWI can nucleate MTs in vitro (Fig. S2 D).

Because ISWI is a RanGTP-dependent MAP (Fig. 1 E), it was possible that RanGTP could also regulate the MT assembly by ISWI. To examine this, we immunoprecipitated ISWI from a *Xenopus* cytostatic factor–arrested metaphase egg extract (CSF extract) using antibodies against full-length ISWI (Fig. 3 A) and tested the MT promoting activity of the immunoprecipitates in the presence and absence of RanQ69L (Fig. 2 D). ISWI immunoprecipitates did not induce MT assembly in 20-μM tubulin solutions, but they did upon addition of RanQ69L (Fig. 2 D). This suggested that the importin-α/β heterodimer might coprecipitate with ISWI. It had been reported that ISWI is coimmunoprecipitated with several polypeptides from *Xenopus* CSF extracts (MacCallum et al., 2002), and our immunoprecipitates showed similar band patterns (Fig. 2 E). Indeed, we identified importin-α and -β in the immunoprecipitates by immunoblot (Fig. 2 E). The interactions are specific because importin-α and -β did not coprecipitate with ISWI from the extracts supplemented with RanQ69L (unpublished data). These results indicated that ISWI nucleates, stabilizes, and bundles MTs in vitro, and the activities are up-regulated by RanGTP.

The ATPase activity of ISWI is not necessary for its effect on MTs

ISWI is an ATPase, the activity of which is essential for chromatin remodeling (Corona et al., 1999). To examine whether the ATPase activity of ISWI was important for its effect on MTs, we prepared a *Xenopus* ISWI mutant in which lysine 204 was replaced with arginine (K204R; Fig. S3 A). This residue was located in a conserved ATP-binding site (GXGKT) and the corresponding mutation in *Drosophila* ISWI abolished its ATPase activity as well as nucleosome remodeling (Corona et al., 1999). In fact, the K204R mutant did not show ATPase activity (Fig. S3 B). Nevertheless, the K204R mutant bound and assembled MTs with the same efficiency as the wild-type protein (Fig. S3, C and D). Moreover, we examined whether the addition of ATP or AMPPNP affected the MT binding or polymerization activities of wild-type ISWI, but it did not affect either activity. These results indicated that the MT-regulating activity of ISWI does not require its ATPase activity in contrast to the chromatin-remodeling activity.

ISWI localizes to the mitotic spindle and chromosomes

To examine the subcellular localization of endogenous ISWI, we prepared three independent ISWI antibodies that specifically recognize ISWI in *Xenopus* XL177 cell lysates (Fig. 3 A) and performed immunofluorescence staining of the cells using a mixture of all three antibodies (Fig. 3 B). In interphase, ISWI was localized in nuclei (Fig. 3 B). In prometaphse, after nuclear envelope break down, ISWI signal on the centrosomes increased, and some ISWI stayed on chromosomes while the rest was distributed throughout the mitotic cytoplasm. In metaphase the centrosome staining further increased and ISWI also became visible on spindle MTs (Fig. 3 B). In anaphase, ISWI remained localized on spindle poles and MTs, and both signals started to decrease at late anaphase (Fig. 4 B; unpublished data). The centrosomal signal decreased further in telophase while ISWI reentered the newly formed nuclei.

We also added GFP-ISWI to *Xenopus* egg extracts to examine its localization during the cell cycle (Fig. 3 C). In interphase extracts, GFP-ISWI was localized inside the nucleus (Fig. 3 C), as expected. The localization of ISWI drastically changed during progression toward mitosis. During the early stages of spindle assembly, GFP-ISWI was detected on chromosomes and along the length of spindle MTs, while none was visualized at the formed spindle pole (Fig. 3 C, 10 min; Yokoyama et al., 2008). The majority of GFP-ISWI then became localized at spindle poles in metaphase, while some were still detected on spindle MTs and chromosomes (Fig. 3 C). In anaphase, GFP-ISWI remained bound to them during chromosome segregation, although ISWI localization on spindle MTs apparently increased (Fig. 3 C). Immunofluorescence staining of egg extract spindles showed the same localization (Fig. 3 D).

Our results in culture cells and egg extracts are consistent with previous reports showing that the majority of ISWI dissociates from chromatin during the cell cycle progression from interphase to mitosis (Demeret et al., 2002; MacCallum et al., 2002). Thus, ISWI binds spindle MTs in mitosis, whereas it stays inside the nucleus during interphase and therefore does not bind cytoplasmic MTs.

ISWI binds to RanGTP spindles and RanGTP-stabilized centrosomal asters

We then tested whether RanGTP could regulate the interaction of ISWI with spindle poles and MTs. To address this possibility, we examined the localization of ISWI protein on RanQ69L-induced pseudo spindles and asters (Carazo-Salas et al., 1999). Both GFP-ISWI addition and immunofluorescence staining showed that ISWI localizes on those structures (Fig. 4, A and B). Moreover, centrosomal asters in CSF extracts did not incorporate GFP-ISWI, but they did when stabilized to form bigger asters in the presence of RanQ69L (Fig. 4 C; Carazo-Salas et al., 2001; Yokoyama et al., 2008). Thus, ISWI binds to spindle poles and MTs in the absence of chromatin, most likely in a RanGTP-dependent manner.

ISWI is required to maintain spindle microtubules in anaphase and for chromosome segregation

We then examined the role of ISWI in cell cycle progression using *Xenopus* egg extracts. Previous work had shown that the depletion of ISWI from egg extracts did not affect DNA replication, chromosome condensation, sister chromatid cohesion, or chromatin decondensation (Demeret et al., 2002; MacCallum et al., 2002), but the role of ISWI in MT organization had not been examined. The addition of the full-length ISWI antibody to interphasic extracts did not inhibit the decondensation of sperm chromatin during nuclear assembly (Fig. 5 A). In metaphase extracts, spindles also assembled normally in the presence of the antibody with condensed chromosomes properly aligned on the metaphase plate (Fig. 5 A). However, subsequent chromosome segregation was strongly inhibited. 10 min after calcium addition, spindle shapes still remained, but the amount of MTs was clearly decreased compared with control extracts (Fig. 5, A and B).

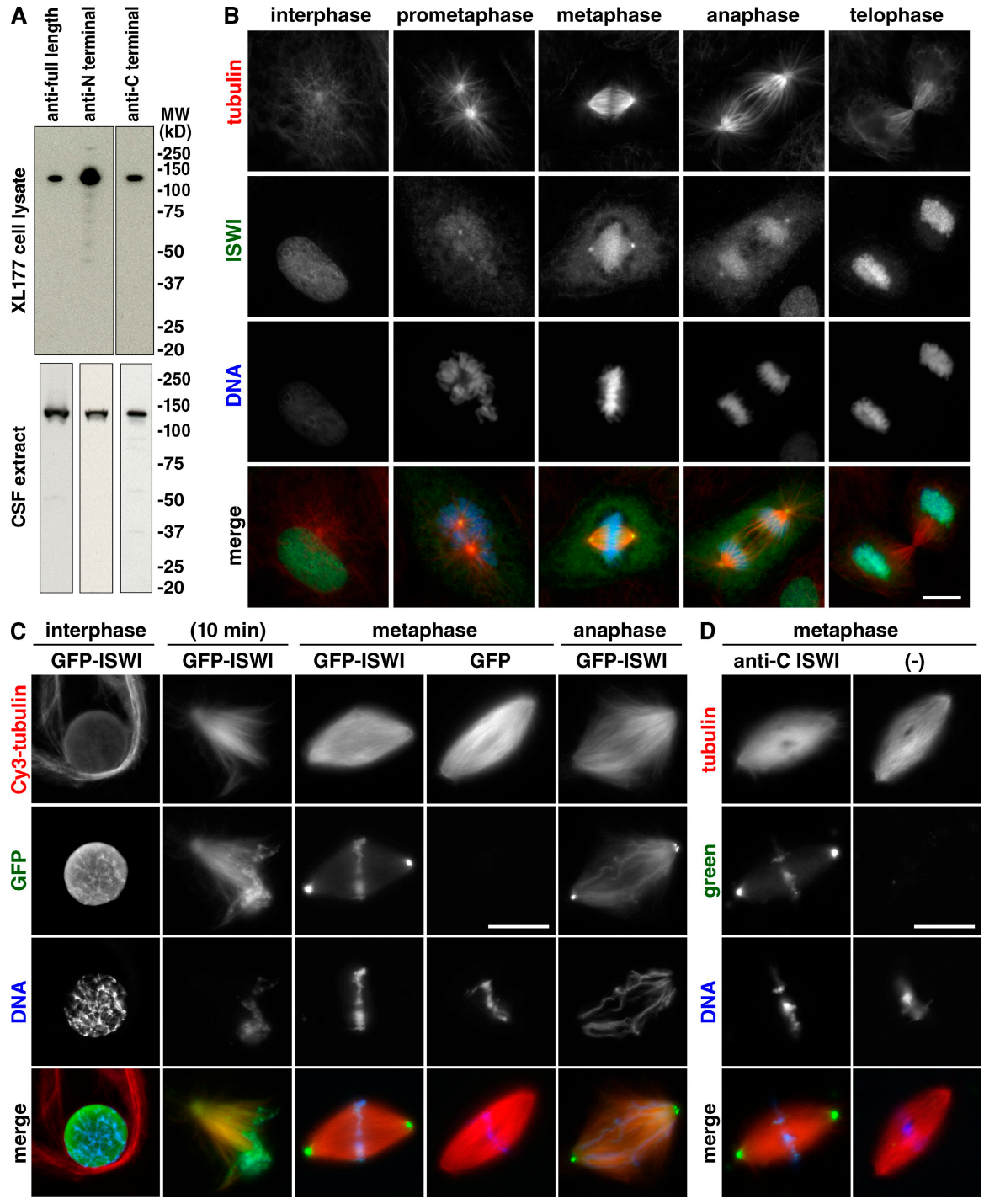

Figure 3. **ISWI localizes in interphasic nuclei and on mitotic spindles in *Xenopus* culture cells and egg extracts.** (A) Immunoblot of *Xenopus* XL177 cell lysate and CSF extract with 1 μg/ml of affinity-purified ISWI antibodies against full-length (1–1046 aa), N-terminal (1–400 aa), or C-terminal (746–1046 aa). (B) Localization of endogenous ISWI in *Xenopus* XL177 cells. Cells were fixed in cold methanol. ISWI was stained with a mixture of the three ISWI antibodies (total 3 μg/ml of each 1 μg/ml) and subsequently with Alexa 488–labeled anti–rabbit IgG (green). Tubulin was stained with anti-tubulin and Alexa 568–labeled anti–mouse IgG (red). DNA was stained with Hoechst 33342 (blue). Bar, 10 μm. (C) Localization of recombinant ISWI in *Xenopus* egg extracts. A CSF extract was immunodepleted with anti–N-terminal ISWI antibody or rabbit IgG, and 1.0 μM GFP-ISWI and GFP control (green) were added back to the extract, respectively. Each extract was supplemented with sperm nuclei and Cy3-labeled tubulin (red), and sent to interphase by adding calcium and incubating at 20°C for 90 min. The samples were cycled into metaphase by adding ISWI- or mock-depleted CSF extract and incubating at 20°C for 60 min, respectively. The samples were further cycled to anaphase by calcium addition and 30 min incubation. At each step, small aliquots were fixed, spun down onto coverslips, and stained with Hoechst (blue). Bar, 20 μm. (D) Endogenous ISWI localizes on mitotic spindles in egg extracts. Cycled sperm spindles were fixed, spun down on coverslips, and stained with or without 1 μg/ml anti–C-terminal ISWI antibody. The coverslips were subsequently stained by Alexa 488–labeled anti–rabbit IgG (green). MTs are red and DNA is blue. Bar, 20 μm.

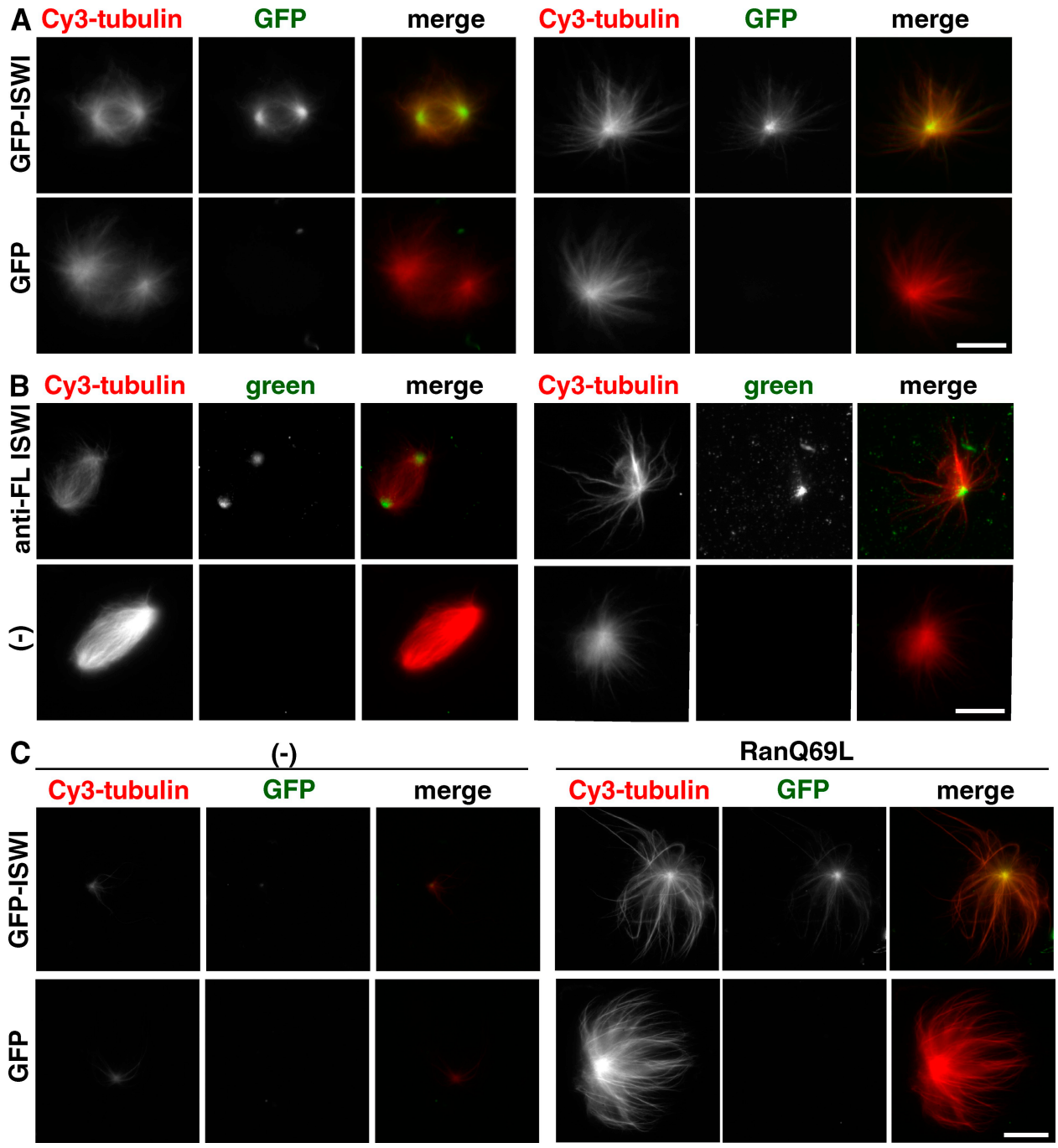

Figure 4. **ISWI binds to RanGTP-induced asters/spindles and RanGTP-stabilized centrosomal asters.** (A) GFP-ISWI is incorporated into poles and MTs of RanGTP-induced asters and spindles. A CSF extract containing 1.3 µM GFP-ISWI or GFP was incubated with RanQ69L and Cy3-tubulin at 20°C for 30 min. The samples were fixed and spun down to coverslips. Bar, 10 µm. (B) Endogenous ISWI localizes to the poles and MTs of the Ran asters/spindles. The RanGTP-nucleated asters and spindles were stained by anti–full-length ISWI antibody and Alexa 488–labeled anti–rabbit IgG (green). Bar, 10 µm. (C) GFP-ISWI is incorporated into RanGTP-stabilized centrosomal asters. A CSF extract containing 1.3 µM GFP-ISWI or GFP control was incubated with centrosomes, anti-TPX2 antibody, and Cy3-tubulin in the presence or absence of RanQ69L at 20°C for 30 min. Anti-TPX2 antibody inhibits RanGTP-dependent MT nucleation. The samples were fixed and spun down on coverslips. Bar, 20 µm.

At 20 min, spindles started to disappear and chromosomes remained clustered in one single structure, whereas they were already segregated in control spindles (Fig. 5, A– C). After 30–40 min, MTs disappeared completely and chromosomes did not segregate, whereas in the control extracts MTs were still present around the segregating chromosomes (Fig. 5, A and B). In the presence of ISWI antibodies, the nonsegregated chromosomes still decondensed after 1 h, as in control extracts (Fig. 5 A). In both extracts, inactivation of histone H1 kinase activity proceeded with identical timing after calcium addition (Fig. 5 D), indicating that cell cycle progression was not affected by the ISWI antibody addition. Similar results were obtained when antibodies were added just before inducing metaphase or anaphase and in extracts from which ISWI was immunodepleted (Fig. S4, A and B).

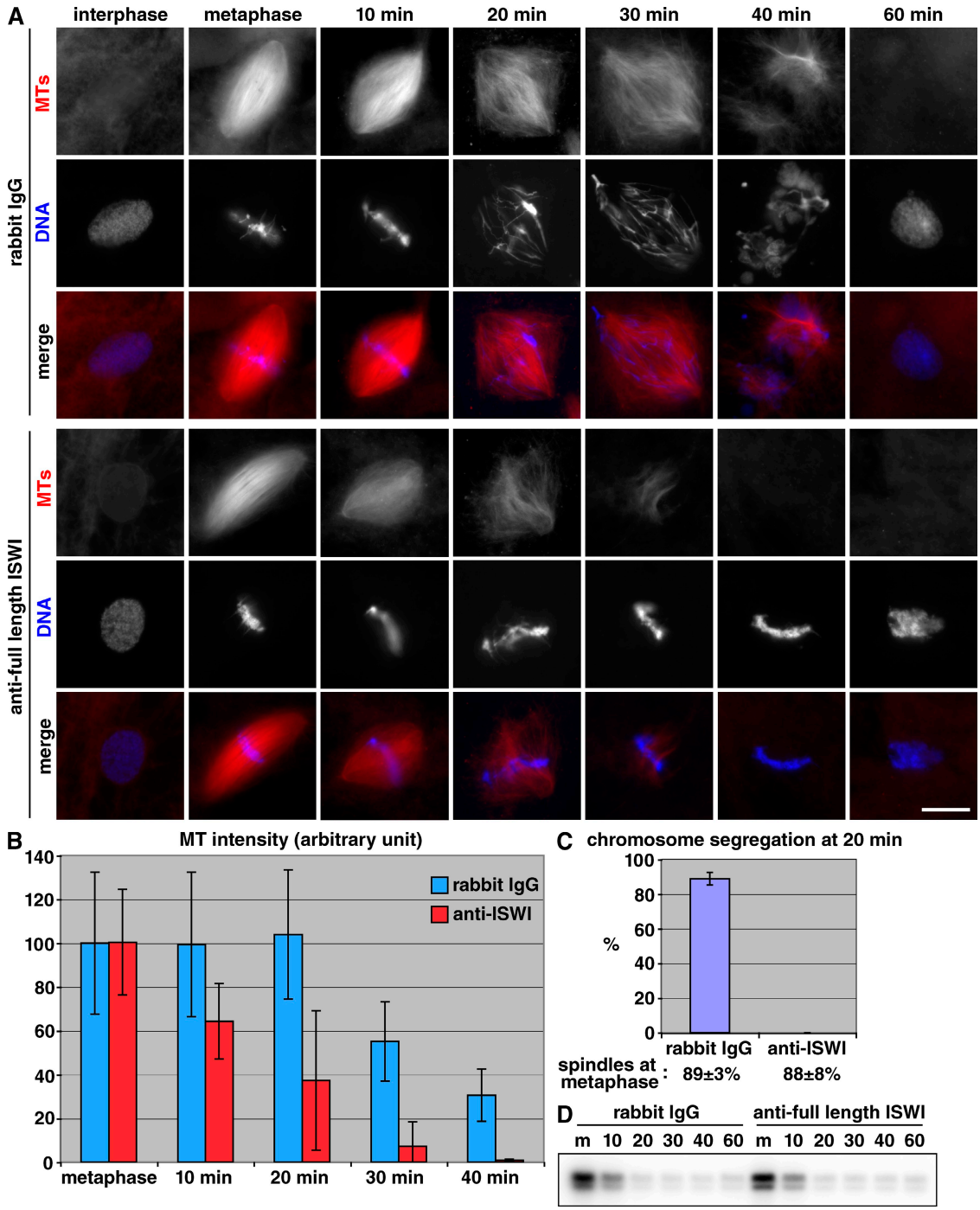

Figure 5. **ISWI is required for the maintenance of spindle MTs in anaphase and chromosome segregation.** (A) A CSF extract was supplemented with 0.37 mg/ml rabbit IgG or anti–full-length ISWI antibodies. Each extract was incubated with sperm nuclei, Cy3-tubulin, and calcium at 20°C for 90 min (interphase). The samples were cycled into mitosis by adding fresh CSF extract and incubating at 20°C for 60 min (metaphase). They were further cycled into anaphase and interphase by adding calcium and incubating at 20°C for 60 min. At each time point, small aliquots were fixed on coverslips by squashing. This experiment was reproduced six times. Bar, 20 µm. (B) MTs disappear at anaphase onset in the presence of ISWI antibody. Spindle assembly and anaphase reactions were performed as described in A, but the samples were then fixed and spun down onto coverslips. The MT intensity around the sperm was quantified using a macro. $n > 40$ structures; $n = 2$ experiments. Error bars represent SD. (C) Chromosomes do not segregate in the presence of ISWI antibody. 20 min after anaphase onset, the percentage of the spindles with segregated chromosomes was quantified over the total number of structures counted. $n = 300$ spindles; $n = 3$ experiments. Error bars represent SD. (D) Cell cycle progression is normal in the presence of ISWI antibody. Histone H1 kinase activity was assayed in metaphase extracts (m), and 10, 20, 30, 40, and 60 min after calcium addition.

In those experiments, calcium was used to induce the transition from metaphase to anaphase. Because calcium is also known to depolymerize MTs, we wondered whether the observed phenotype reflected anaphase onset or a general MT destabilization caused by calcium. To address this, we induced anaphase by adding calcium/calmodulin-dependent kinase II (CaMKII) to the metaphase-arrested extracts (Hannak and Heald, 2006; Reber et al., 2008). In the presence of ISWI antibodies,

spindle MTs still disappeared at anaphase onset and chromosomes did not segregate (Fig. S4, C and D). Thus, ISWI is required for the stability of anaphase spindle MTs and chromosome segregation, but not for chromosome condensation, spindle assembly, chromosome alignment on the metaphase plate, or chromosome decondensation.

Because ISWI is a chromatin-remodeling complex protein, it might have been involved in some aspect of chromosome separation in anaphase. To address this possibility, we examined the effect of ISWI inactivation on spindles assembled around plasmid DNA–coated beads (Heald et al., 1996). The DNA bead spindles do not have kinetochores and do not segregate in anaphase. When anaphase was induced by calcium addition to control extracts, spindles remained intact over 20 min before dissociating without performing anaphase elongation movements (Fig. 6 C). In ISWI-depleted extracts (Fig. 6 A), spindles assembled properly in metaphase, but they disappeared rapidly 5 min after calcium addition (Fig. 6, C and D). Spindle MTs seemed to depolymerize evenly rather than at any specific site (Fig. 6 C). Addition of recombinant ISWI to the depleted extracts rescued the phenotype (Fig. 6, C and D). In all three extracts, histone H1 kinase activity decreased with exactly the same timing (Fig. 6 E). Thus, in ISWI-depleted extracts, MTs depolymerize at anaphase onset independently of kinetochore assembly and chromosome segregation.

These results indicated that in contrast to other known RanGTP-dependent MAPs (Kalab and Heald, 2008), ISWI is not essential for spindle assembly, but it is required to maintain MT stability during anaphase, and this is essential for chromosome segregation.

ISWI maintains spindle microtubules during anaphase independently of its role in chromatin remodeling

Because spindles assembled around sperm nuclei or DNA beads containing chromatin, we could not formally exclude the possibility that ISWI requirement in anaphase was mediated through its potential chromatin-remodeling activity. Therefore, we analyzed the stability of RanGTP spindles in anaphase, which do not contain chromatin. In control extracts, the spindle-like structures disappeared quickly, 5–10 min after calcium addition (Fig. S5), consistent with the previous report (Reber et al., 2008). The lifetime of RanGTP spindles (~10 min) in anaphase was much shorter than that of sperm and DNA bead spindles (~40 min; Fig. 5; Fig. 6; Fig. S5). The addition of excess recombinant ISWI (4 μM) did not affect the number and the shape of the RanGTP spindles in CSF extracts, but it maintained the spindle-like structures during anaphase (~40 min; Fig. S5). The spindles were then disassembled as the extract state changed to interphase (Fig. S5 B). Smaller concentrations of ISWI (<1.4 μM) did not prolong the lifetime of Ran spindles. These results indicated that in anaphase ISWI stabilizes spindle MTs as a MAP, but this process does not require the chromatin-remodeling activity of ISWI.

ISWI is required for RanGTP-dependent microtubule stabilization in anaphase

The results reported above suggested that ISWI might regulate MT stability in anaphase in a RanGTP-dependent manner. To address this, we examined the stability of MTs nucleated by centrosomes during anaphase in the presence or absence of RanQ69L (Fig. 7). In control extracts in the absence of RanQ69L, astral MTs remained short and dynamic at 20 min after calcium addition, and then they changed into long MTs at 60 min as the interphase state was established (Fig. 7). RanQ69L clearly stabilized MTs in the anaphase extracts (20 min), although the stabilization effect was weaker than that in CSF extracts (Fig. 7). This result indicated that RanGTP stabilizes MTs in anaphase, whereas it does not nucleate MTs, as shown in Fig. S5. The addition of the ISWI antibody did not affect the RanGTP-dependent MT stailization in CSF extract, but specifically inhibited MT stabilization in anaphase (Fig. 7). Thus, RanGTP stabilizes MTs in anaphase by activating ISWI.

ISWI is required for cell growth, anaphase microtubule stability, and chromosome segregation in *Drosophila* S2 cells

To examine the role of ISWI in vivo and in a different organism, we performed RNAi against ISWI in *Drosophila* S2 cells. We used these cells because *Drosophila* has one ISWI gene, whereas mammals have two. Three independent dsRNAs for ISWI were prepared according to the sequence information on the Genome RNAi database (Horn et al., 2007). Treatment of S2 cells with the dsRNAs efficiently down-regulated the protein level of ISWI after 2 d, in comparison to cells treated with control dsRNA for GFP (Fig. 8 A, day 4).

ISWI-depleted cells, treated with all three dsRNAs, grew slowly and eventually stopped growing (see Fig. 10 B). FACS analysis at 4 d did not show a difference between control and ISWI-depleted cells. After 12 d, however, ISWI-depleted cell populations contained more G2/M phase cells and a decreased level of S phase cells (Fig. 8 C; Table I). Cells with less than 2N chromosomes increased also, indicating the occurrence of apoptotic and/or aneuploid cells (Fig. 8 C; Table I).

To examine spindle morphology and chromosome segregation, the cells were immunostained for tubulin and DNA after 4 d (Fig. 8, D and E). In control cells, spindles elongated when chromosomes were segregated at anaphase (Fig. 8 D). In ISWI-depleted cells (MRC015_H12), we found mitotic cells that did not exist in the control. They were classified into four phenotypes and the proportion of each phenotype in the total mitotic cells was quantified (Fig. 8 E; Table II). Longer spindles were seen with chromosomes staying in the central region (phenotype 1; 6.7 ± 1.8%). Most frequently, we detected longer spindles with one or more chromosomes separated and located close to the spindle poles (phenotype 2; 17.9 ± 5.6%). In these two phenotypes, the morphology of the spindle MTs seemed to be normal. We also observed longer defective spindles or apparently shrinking spindles having chromosomes scattered through the spindle (phenotype 3; 2.9% ± 0.1%). Furthermore, anaphase or telophase spindles, judged by chromosome separation, were found with defective MTs and chromosomes lagging or missegregating (phenotype 4; 7.4 ± 6.5%). In phenotypes 3 and 4, MTs were often detached from the spindles together with chromosomes, but still connected to spindle poles (Fig. 8 E, arrows). Mitotic indices were not affected in ISWI-depleted cells for at

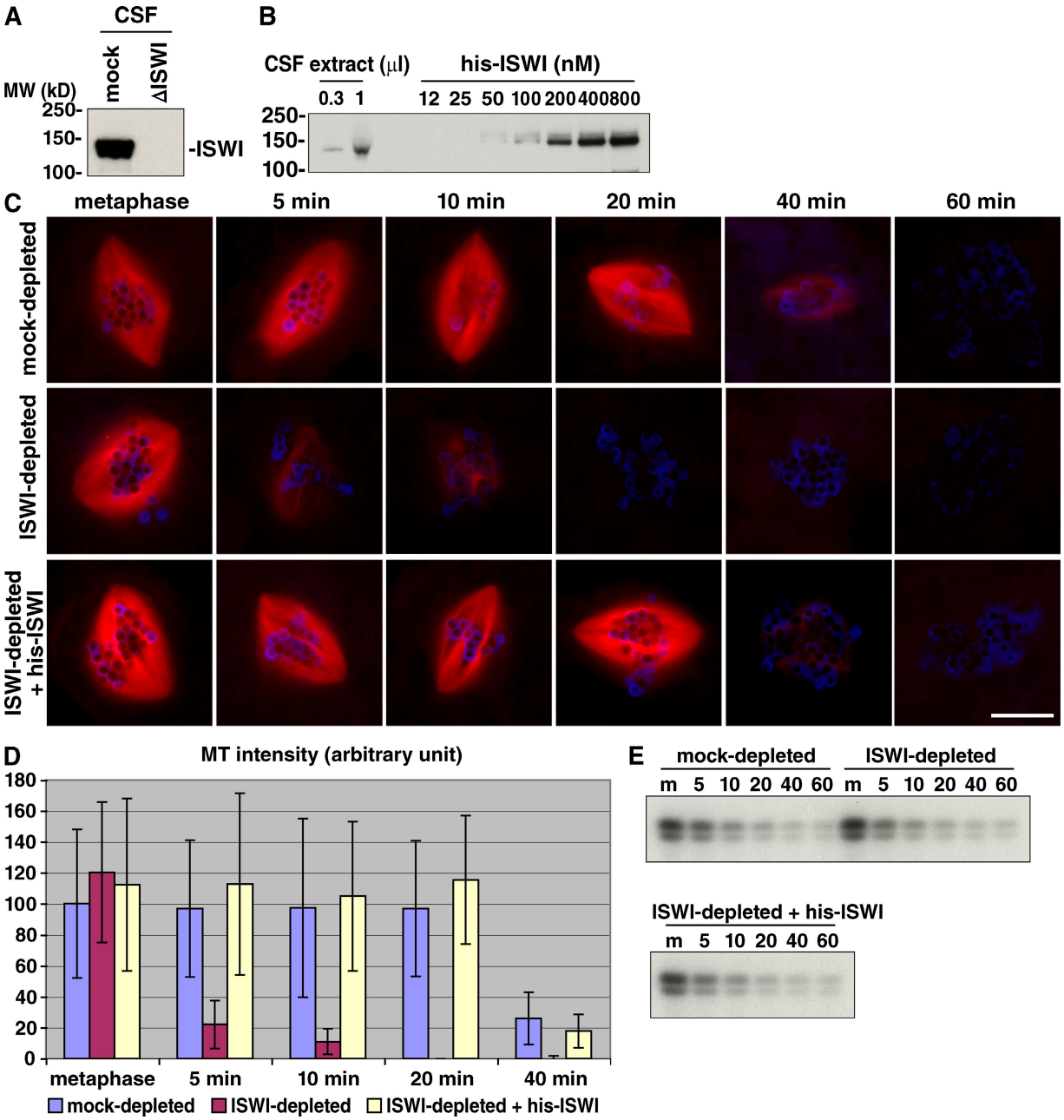

Figure 6. **ISWI is required to stabilize spindle MTs in anaphase independently of chromosome segregation.** (A) Immunodepletion of ISWI. A CSF extract was immunodepleted using rabbit IgG or anti–N-terminal ISWI antibodies. Each extract (1 μl) was immunoblotted by anti–N-terminal ISWI antibodies. (B) Determination of endogenous concentration of ISWI in *Xenopus* CSF extracts. A CSF extract (0.3 μl and 1.0 μl) and recombinant ISWI (1.0 μl from described concentrations) was loaded on an SDS-PAGE gel and immunoblotted with anti–N-terminal ISWI antibodies. We estimate that the endogenous concentration is ~200 nM. (C) Spindle MTs disappear at anaphase onset in the absence of ISWI that is restored by recombinant ISWI. The mock or ISWI-depleted extracts were supplemented with DNA beads and Cy3-tubulin, and cycled into interphase and then back into mitosis. The metaphase extracts containing DNA bead spindles were sent to anaphase by calcium addition. At each time point, small aliquots of the samples were fixed on coverslips by squashing. Recombinant ISWI (1 μM) was added back to ISWI-depleted extracts before the reactions. This experiment was reproduced four times. Bar, 20 μm. (D) Quantification of the MT amounts around DNA beads assayed in C. MT intensity around DNA bead clusters containing 10–40 beads was quantified using a macro. Note that the clusters containing 10–40 beads mostly formed bipolar spindles in metaphase extracts, whereas the clusters with less than 10 beads did not nucleate MTs and the clusters with more than 40 beads formed multipolar spindles. Error bars represent SD. $n > 40$ structures; $n > 2$ experiments. (E) Cell cycle progression is normal in ISWI-depleted extract. Histone H1 kinase activity was assayed in metaphase (m), and 10, 20, 30, 40, and 60 min after calcium addition.

least 4 d (Table II). The proportions of prophase, prometaphase, and metaphase in ISWI-depleted cells were similar to those in control cells, but the proportions of proper anaphase and telophase decreased in ISWI-depleted cells (Table II). The other two dsRNAs for ISWI (HFA07446 and OB2651) showed the same phenotypes with similar frequencies, indicating that the observed defects were caused by the lack of ISWI.

To address directly whether ISWI is required in anaphase, we conducted live-cell imaging of S2 cells stably expressing GFP–α-tubulin and mCherry-centromere identifier

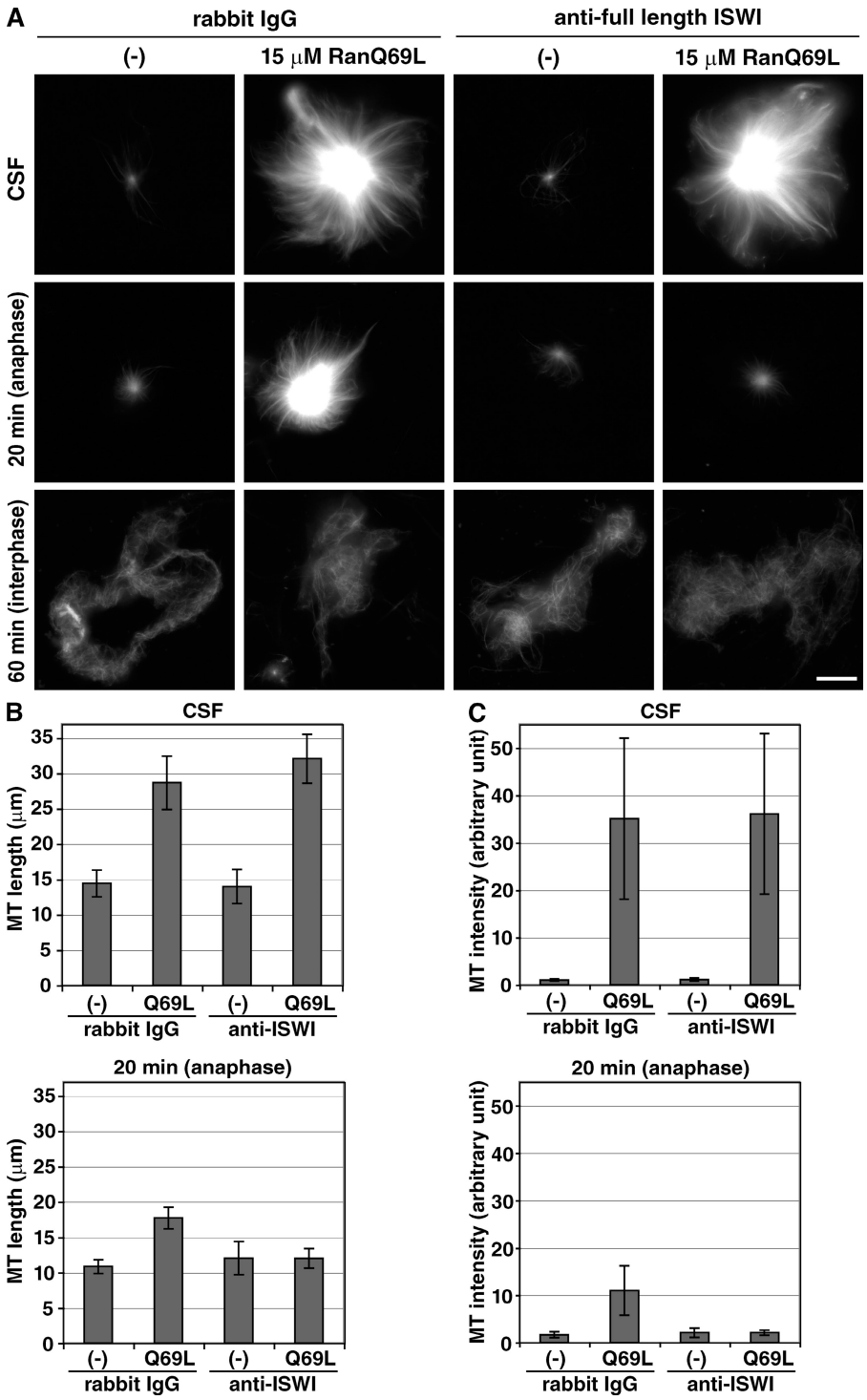

Figure 7. **RanGTP stabilizes MTs in anaphase and ISWI is required for MT stabilization.** (A) A CSF extract was supplemented with 0.37 mg/ml rabbit IgG or anti–full-length ISWI antibody. The CSF extracts were incubated with centrosomes, anti-TPX2 antibody, and Cy3-tubulin in the presence or absence of RanQ69L at 20°C for 30 min. The samples were then cycled into anaphase and interphase by calcium addition. At each time point, the samples were fixed, spun down on coverslips, and imaged. This experiment was reproduced three times. Note that the MT stabilization assay is performed in the presence of anti-TPX2 antibody that inhibits RanGTP-dependent MT nucleation and thus keeps the number of asters constant during the assay. This is important to evaluate MT stabilization activity correctly (Yokoyama et al., 2008). Bar, 20 μm. (B) Quantification of the MT length of centrosomal asters assayed in A as described previously (Yokoyama et al., 2008). Error bars represent SD; $n > 20$ asters. (C) Quantification of the MT intensity of centrosomal asters assayed in A. Error bars represent SD; $n > 20$ asters.

(CID, a kinetochore marker; Coelho et al., 2008) at 4 d after dsRNA treatment (Fig. 9; Videos 1–3). We found normal metaphase spindles in ISWI RNAi cells with similar frequency to control cells, consistent with our quantitation of fixed cells (Table II). When we filmed the metaphase cells to follow their cell cycle progression, however, the spindles in ISWI-depleted cells frequently disintegrated and chromosomes did not segregate during an imaging period of 1 h (7 out of 12 cells filmed; Fig. 9 B; Videos 2 and 3). Before the MTs disintegrated, sister chromatids separated and moved slightly poleward (Fig. 9 B; Videos 2 and 3), suggesting that the cells entered anaphase (Matos et al., 2009). Spindles then became longer until they reached the plasma membranes, and MTs were detached from spindles with chromosomes or started to shrink (Fig. 9 B; Videos 2 and 3).

This demonstrates that ISWI is essential for *Drosophila* cells to grow and progress from G2/M phases, and is required for anaphase MT stability and chromosome segregation. Thus, the significant role of ISWI in anaphase is conserved in *Drosophila*.

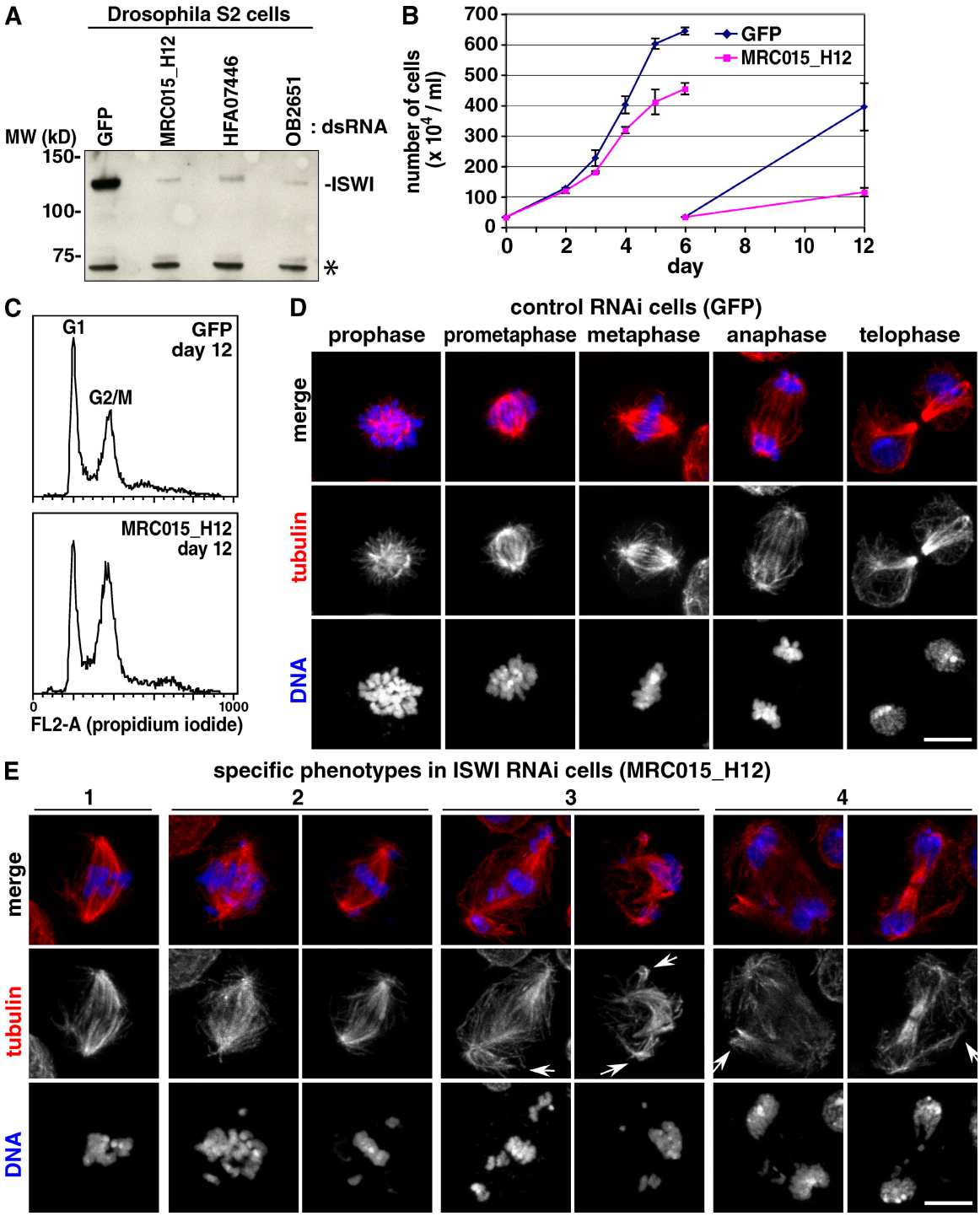

Figure 8. **ISWI is required for cell growth, anaphase MT stability, and chromosome segregation.** (A) ISWI is down-regulated by dsRNAs in *Drosophila* S2 cells. Cells were treated with described dsRNAs for 4 d. The cells (each 5 × 10^4 cells) were loaded on a gel and immunoblotted using anti–N-terminal *Xenopus* ISWI antibody. *, nonspecific band and loading control. (B) ISWI-depleted cells stop growing. After transfection with described dsRNAs (d 0), the number of the cells was counted using a hemocytometer at the day indicated. At 6 d, the confluent cells were diluted to 0.33 × 10^4 cells/ml and further incubated with fresh dsRNAs. Error bars represent the SD of two independent experiments. (C) ISWI-depleted cells accumulate in G2/M phases. S2 cells were treated with the described dsRNAs for 12 d, stained with propidium iodide, and analyzed by FACS. (D) Mitotic cells detected in control RNAi cells. At 4 d after dsRNA treatment for GFP, the cells were fixed and stained for tubulin (red), DNA (blue) and phopho-histone H3 (green). Mitotic cells, identified by the mitotic specific phospho-histone H3 signal, were analyzed using a confocal microscope. The images projected with maximum intensity are presented. (E) Abnormal mitotic cells specifically found in ISWI-depleted cells. At 4 d after dsRNA treatment for ISWI (MRC015_H12), the cells were fixed, stained, and analyzed using a confocal microscope. The abnormal spindles were classified into four phenotypes. (1) Longer spindles with chromosomes staying in the center region. (2) Longer spindles with chromosomes mainly staying in the center but some locating close to poles. (3) Longer defective spindles or shrinking spindles having chromosomes scattered through the spindle. (4) Anaphase or telophase spindles judged by chromosome separation with defective MTs and chromosomes lagging or missegregating. In phenotype 3 and 4, MTs were often displaced from spindles by accompanying chromosomes, but were still connected to spindle poles (arrows). Bars, 5 μm.

Table I. **Quantification of cell cycle stages in control or ISWI RNAi S2 cells at 12 d[a]**

	<G1[b]	G1	S	G2/M	>G2/M[c]
Control RNAi (GFP)	0.2 ± 0.2	25.6 ± 1.8	32.6 ± 10.5	25.6 ± 2.1	15.6 ± 6.7
ISWI RNAi (MRC015_H12)	1.0 ± 0.1	19.6 ± 1.6	30.1 ± 5.7	34.2 ± 3.0	14.5 ± 3.7

[a]Values represent the percentage of each cell cycle phase over the total number of cells. The cells at 12 d after dsRNA treatment were stained with propidium iodide and analyzed by FACS. The percentage of each phase was calculated from the FACS profiles (Fig. 10 C; unpublished data) using the FlowJo software (Tree Star, Inc.) following the Watson Pragmatic model (Watson et al., 1987). Errors represent SD from two (control RNAi) and three (ISWI RNAi) independent experiments, respectively.

[b]<G1: cells with less than 2N chromosomes.

[c]>G2/M: cells with more than 4N chromosomes.

Discussion

ISWI is a bona-fide MAP regulated by RanGTP

We identified a known chromatin remodeling factor, ISWI, as a potential NLS-MAP by sequential affinity purification of NLS proteins and MAPs. In vitro, ISWI binds to pure MTs with high affinity and decorates the lattice of MTs with a likely stoichiometry of one ISWI per one tubulin dimer. The MT binding of ISWI is specifically inhibited by the importin-α/β heterodimer and the inhibition is reversed by RanGTP. ISWI bundles preexisting MTs and induces MT assembly from pure tubulin, often forming MT asters. The ISWI-dependent MT assembly is also positively regulated by RanGTP in vitro. Consistently, ISWI accumulates on spindle MTs during mitosis in *Xenopus* culture cells and egg extracts, and is required for RanGTP-dependent MT stabilization during anaphase in extracts. These results demonstrate that ISWI is a bona-fide nuclear MAP regulated by RanGTP and suggest that analysis of all the protein bands found in the NLS-MAP fraction will lead to the identification of additional MAPs that function locally around chromosomes during mitosis.

Chromatin-remodeling activity and microtubule-regulating activity of ISWI

ISWI is one of the ATPases included in chromatin-remodeling complexes (Brown et al., 2007). The fundamental function of the complexes is to slide nucleosomes along the DNA in order to make specific DNA sequences accessible or inaccessible to regulators. Each complex contains one ATPase, and the ATPase activities are essential for the complexes to mobilize nucleosomes (Corona et al., 1999). Currently, the catalytic ATPase subunits fall into three families, the SWI/SNF family, the ISWI family, and the CHD family (Brown et al., 2007). The three families of ATPase subunits have distinct roles and exhibit homology restricted to the ATPase domain (Brown et al., 2007). Among them, only ISWI has been reported to bind MTs (Trachtulcová et al., 2000; Liska et al., 2004). In this study, we demonstrated that the ATPase activity of ISWI is not necessary for its MT binding and assembly activities in vitro, indicating that the chromatin-remodeling and MT-regulating activities are distinct. SANT and SLIDE domains specifically contained in ISWI could be important for the MT-regulating activity (Grüne et al., 2003).

Physiological function of ISWI

Although the role of ISWI in chromatin remodeling has been established in vitro, the function of ISWI in vivo remained unclear. In *Drosophila*, null ISWI mutants die in late larval stages when the maternal contribution of ISWI is depleted (Deuring et al., 2000). In mammals, there are two ISWI genes (SNF2H and SNF2L). SNF2H is mainly expressed in proliferating cells, whereas SNF2L is expressed in differentiated cells (Lazzaro and Picketts, 2001). SNF2H-null mice are embryonic lethal (Stopka and Skoultchi, 2003). In *Xenopus laevis*, only one ISWI is known, which is expressed primarily during development and poorly detectable in adult differentiated tissues (Demeret et al., 2002). Down-regulation of the ISWI protein in *Xenopus* embryos inhibited their early development (Dirscherl et al., 2005). These results suggest that ISWI is essential for cell growth, differentiation, or viability, but do not clarify which cellular process ISWI is required for.

Previously in *Xenopus* egg extracts, immunodepletion of ISWI was shown not to affect nucleosome assembly, DNA

Table II. **Quantification of the mitotic defects in control or ISWI RNAi S2 cells at 4 d[a]**

	Prophase	Prometaphase	Metaphase	Anaphase	Telophase	Mono/multipolar spindles
Control RNAi (GFP)	7.9 ± 2.9	9.9 ± 0.2	23.3 ± 0.4	9.9 ± 1.3	41.1 ± 1.3	6.4 ± 3.4
ISWI RNAi (MRC015_H12)	6.3 ± 0.4	11.2 ± 1.1	23.2 ± 4.5	3.4 ± 0.5	13.6 ± 1.9	7.3 ± 0.4

	1[b]	2[b]	3[b]	4[b]	Mitotic index
Control RNAi (GFP)	1.0 ± 0.1	0	0	0	3.3 ± 0.1
ISWI RNAi (MRC015_H12)	6.7 ± 1.8	17.9 ± 5.6	2.9 ± 0.1	7.4 ± 6.5	3.0 ± 0.9

[a]Values represent the percentage of each mitotic phase or classified phenotype over the total number of mitotic cells. The cells at 4 d after dsRNA treatment were immunostained and counted under a microscope (more than 100 mitotic cells per sample). Errors represent SD from two independent experiments.

[b]Abnormal mitotic cells were classified into four phenotypes (Fig. 10 E).

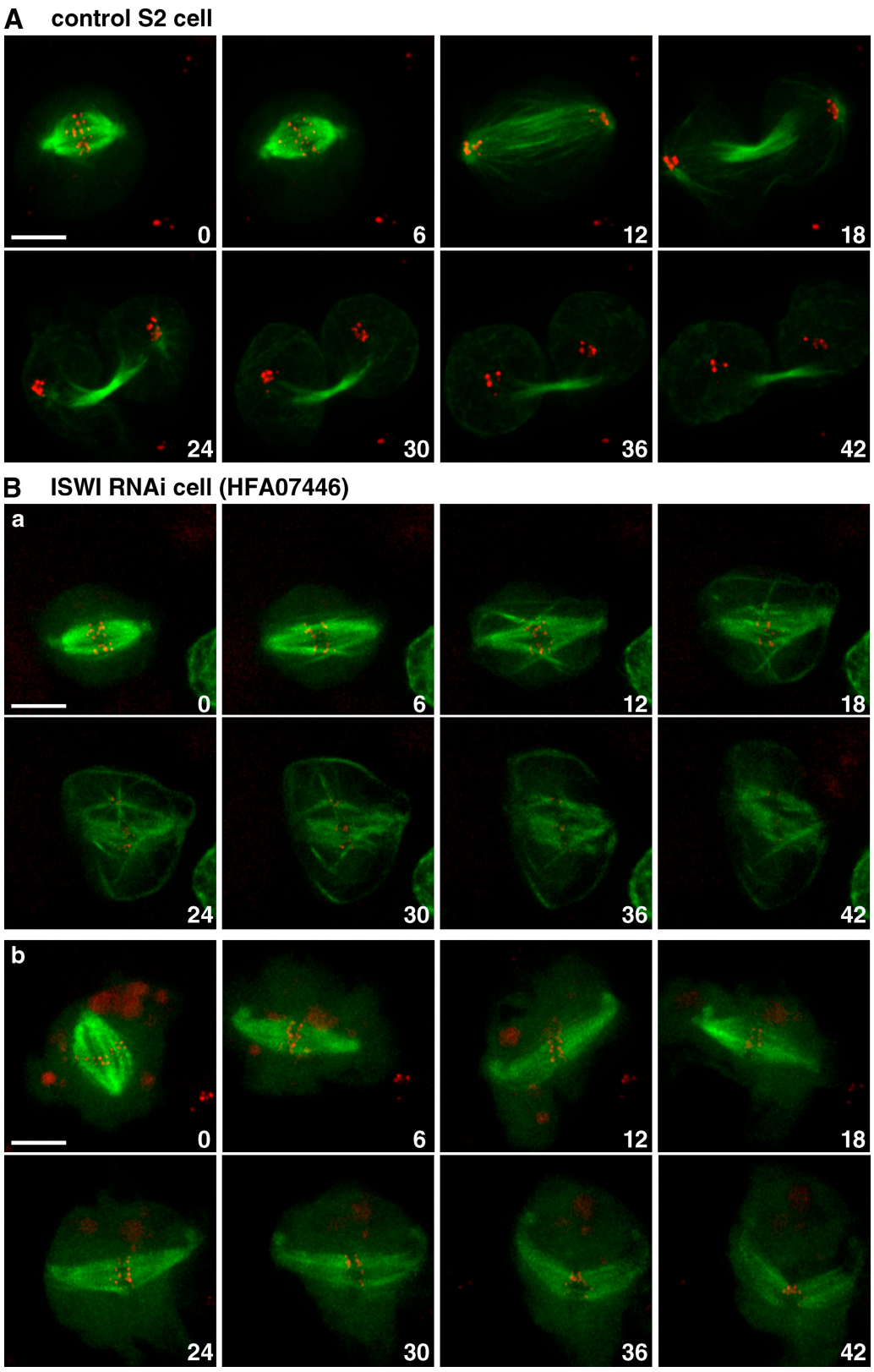

Figure 9. **Live-cell imaging of *Drosophila* S2 cells showing requirement for ISWI in anaphase.** After 4 d of dsRNA treatment, S2 cells stably expressing GFP–α-tubulin (green) and CID-mCherry (red) were filmed to analyze spindle and chromosome dynamics during anaphase. Z stacks of the acquired images were projected with maximum intensity, and stills of the time-lapse analysis are presented. Times in minutes from the start of the video are indicated in each frame. (A) Control S2 cell treated identically but without dsRNA. See Video 1. (B) ISWI RNAi (HFA07446). (a) See Video 2. (b) See Video 3. Bars, 5 μm.

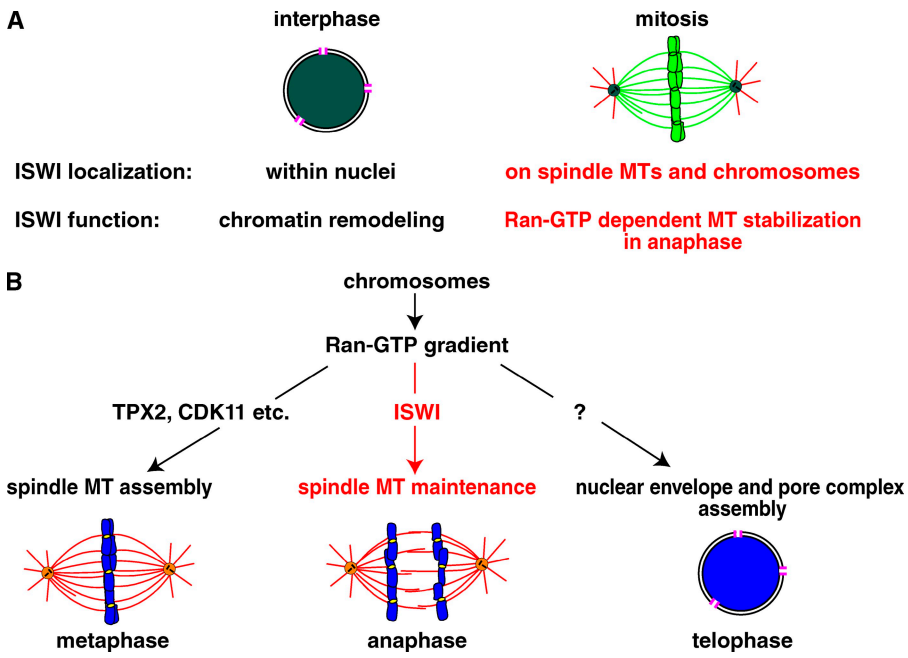

Figure 10. **Models for novel function of ISWI and RanGTP.** (A) A novel role of ISWI in mitosis. In interphase, ISWI localizes inside nuclei and binds to chromosomes for chromatin remodeling. In mitosis, the majority of ISWI dissociates from chromosomes and localizes on spindle poles and microtubules. ISWI is essential for RanGTP-dependent microtubule stabilization in anaphase. (B) A novel role of chromosomes and RanGTP in anaphase. Chromosomes produce RanGTP gradient around them throughout mitosis. RanGTP induces spindle assembly in metaphase and nuclear envelope and pore complex assembly in telophase. Distinctly, RanGTP stabilizes and maintains spindle MTs in anaphase by activating ISWI. This is essential for chromosomes to be segregated along the MTs. Chromosomes and RanGTP probably induce additional events in mitosis in order to ensure chromosome segregation and cell division.

replication, chromosome condensation, sister chromatid cohesion, or chromatin decondensation (Demeret et al., 2002; MacCallum et al., 2002). Consistently, we see no effect on these processes in our ISWI immunodepletion or antibody addition. However, in both types of experiment we observe a significant reduction of MT stabilization in anaphase associated with chromosome segregation defects. In addition, ISWI depletion in *Drosophila* cells results in MT and chromosome segregation defects in anaphase or telophase. And the depleted cells eventually stop growing, with accumulation in G2/M phases. Thus, the critical role of ISWI in anaphase is conserved in different organisms. The lethality observed in null ISWI mutants in *Drosophila* and mouse may be due to the lack of proper chromosome segregation, although this remains to be investigated further.

ISWI localization on spindles during mitosis

It has been reported in *Xenopus* egg extracts that the majority of ISWI dissociates from chromosomes when the cell cycle state of the extract is converted from interphase to mitosis (Demeret et al., 2002; MacCallum et al., 2002). In agreement with this observation, we show that ISWI binds predominantly to chromosomes and partially to MTs at the beginning of spindle assembly, whereas it mainly accumulates on spindle poles during metaphase. Thus, in the process of spindle assembly, ISWI seems to move from chromosomes to spindle microtubules and poles. These localization results suggest that ISWI may function as a chromatin-remodeling ATPase in interphase and as a MAP in mitosis (Fig. 10 A).

Specific requirement of ISWI in anaphase

ISWI is a RanGTP-dependent MAP that localizes to spindle poles and MTs throughout mitosis. Depletion of other known RanGTP-dependent MAPs in extracts or cells results in defects in spindle assembly in metaphase (Kalab and Heald, 2008). However, in ISWI-depleted extracts and ISWI antibody-treated extracts, we only detect defects in MT stability and chromosome segregation during anaphase. In metaphase, spindles assemble with normal kinetics and morphology, and chromosomes are properly aligned on the metaphase plate. The down-regulation of ISWI in *Drosophila* cells also shows clear defects in anaphase but apparently not in prophase, prometaphase, and metaphase. These results therefore indicate that differently from other Ran-regulated MAPs, ISWI is specifically required during anaphase.

On the other hand, we find that RanGTP stabilizes centrosomal MTs in anaphase extracts while it does not nucleate MTs. This is interesting because in metaphase RanGTP induces both stabilization and nucleation of MTs that are essential for spindle assembly (Gruss et al., 2001; Yokoyama et al., 2008). ISWI is required for the RanGTP-dependent MT stabilization in anaphase but not in metaphase. In addition, recombinant ISWI stabilizes and maintains RanGTP spindles during anaphase. Importantly, both assays do not contain chromatin. These results demonstrated that ISWI stabilizes and maintains spindle MTs during anaphase in a RanGTP-dependent manner, and that this process does not require chromatin. The maintenance of spindle MTs in anaphase must be essential for chromosomes to be segregated along the MTs.

The above finding raises the question of why there is a specific requirement for ISWI in anaphase. Although this remains to be investigated, we propose two possibilities. First, ISWI may be activated throughout mitosis by RanGTP, but redundant with other MT stabilization proteins in early steps of mitosis. Indeed, some MAPs required for spindle assembly, like TPX2 and HURP, undergo degradation in anaphase (Hsu et al., 2004; Stewart and Fang, 2005). Because of this, ISWI function in anaphase may be no longer redundant, but essential, for the maintenance of spindle MT stability. The second possibility is that ISWI may not have any function in metaphase regardless of its binding to spindles and may only be activated in anaphase. In that case, ISWI could be regulated by another mechanism, such

as an interacting protein or a modification of ISWI protein, in addition to RanGTP.

In summary, we have shown here that, in addition to its role as a chromatin-remodeling factor, ISWI functions as a RanGTP-dependent MAP required for MT stability in anaphase (Fig. 10 A). Moreover, RanGTP induces spindle assembly at the beginning of mitosis as well as nuclear envelope and pore complex formation at the end of mitosis (Fig. 10 B; Hetzer et al., 2002; Clarke and Zhang, 2008). The present results demonstrate a novel distinct role for RanGTP in chromosome segregation during anaphase, extending the function of chromosomes in mitosis to controlling their own segregation (Fig. 10 B).

Materials and methods

Xenopus egg extract, spindle assembly, anaphase progression, immunodepletion, and antibody addition

Xenopus cytostatic factor–arrested metaphase egg extracts (CSF extracts) were prepared as described previously (Murray, 1991). In brief, *Xenopus* eggs were dejellied by cysteine treatment, washed with XB buffer (10 mM K-Hepes, 100 mM KCl, 1 mM $MgCl_2$, 0.1 mM $CaCl_2$, and 50 mM sucrose, pH 7.7) and subsequently CSF-XB buffer (10 mM K-Hepes, 100 mM KCl, 3 mM $MgCl_2$, 0.1 mM $CaCl_2$, 50 mM sucrose, and 5 mM EGTA, pH 7.7), and crushed by centrifugation at 20,000 *g* for 20 min at 16°C. The straw-colored middle layer was recovered as a CSF extract. DNA bead preparation, cycled spindle assembly, anaphase progression, immunodepletion, and antibody addition were performed as described previously (Hannak and Heald, 2006). In brief, endogenous ISWI was depleted from CSF extracts by 3- or 4-time incubations of 60% (vol/vol) Dynabeads Protein A coupled with anti–full-length or N-terminal ISWI antibodies. Recombinant ISWI was added back to the depleted CSF extracts before sending to interphase. In antibody addition experiments, rabbit IgG (Sigma-Aldrich) or anti–full-length ISWI antibodies were added to CSF extracts at 0.37 mg/ml before sending to interphase. The reactions were squashed or spun down on coverslips, as described previously (Hannak and Heald, 2006). MT intensity around sperm or DNA beads was quantified using a macro written in MatLab (The MathWorks). Histone H1 kinase activity was assayed as described previously (Félix et al., 1990). Constitutively active CaMKII was added as described previously (Reber et al., 2008).

Sequential purification of NLS proteins and MAPs from CSF extracts

NLS proteins were isolated from *Xenopus* CSF extracts as described previously (Yokoyama et al., 2008). In brief, CSF extracts (13.4 ml) were incubated with a 40% wet bead volume (5.36 ml) of z-RanQ69L beads at 4°C for 1 h. The beads were removed by centrifugation, and the extract (activated extract) was incubated with a 120% wet bead volume (16 ml) of GST–importin-β beads at 4°C for 1 h. The beads were separated from the extract (depleted extract) by centrifugation, washed five times with a wash buffer (CSF-XB, 100 mM NaF, 80 mM β-glycerophosphate, 0.1 mM sodium vanadate, 0.03% digitonin, and 1 mM DTT), and incubated with a 75% volume (10 ml) of an elution buffer (20 µM RanQ69L-GTP, 500 mM NaCl, 1 mM GTP, 1 mM ATP, and 10% glycerol in the wash buffer) at 4°C overnight. The eluate (the NLS protein fraction) was dialyzed to CSF-XB supplemented with 10% glycerol and 1 mM DTT.

The NLS protein fraction (10 ml) was incubated with 2 µM taxol-stabilized MTs in the presence of 1 mM GTP and 10 µM taxol at 20°C for 15 min, and the MTs were spun down at 100,000 *g* for 10 min at 20°C through a 40% glycerol cushion in CSF-XB containing 20 µM taxol. The MT pellet was resuspended with a wash buffer (CSF-XB containing 1 mM DTT, 1 mM GTP, and 20 µM taxol) and spun down again through the cushion. The washing was repeated one more time. The MT pellet was incubated with 500 µl of 500 mM NaCl in the wash buffer for 10 min at room temperature, and the MAPs were recovered in the supernatant after centrifugation at 100,000 *g* for 10 min at 20°C.

Cloning and recombinant proteins

A cDNA clone (IMAGE:6317687, RZPD) covering the complete *Xenopus* ISWI cDNA was amplified by PCR and cloned into EheI–HindIII sites of pFastBac HTa (Invitrogen). Baculoviruses were prepared following the manufacturer's instructions. Recombinant ISWI was expressed in Sf21 insect cells, and purified on Talon beads (BD) and a Mono S column (GE Healthcare). GFP-ISWI was prepared as described for ISWI. The K204R mutant of ISWI, in which lysine 204 was replaced with arginine, was constructed by site-directed mutagenesis using PfuTurbo DNA polymerase (Agilent Technologies), and prepared as described for ISWI. N-terminal ISWI (1–400 aa) and C-terminal ISWI (746–1046 aa) were amplified by PCR and cloned into BamHI–XhoI or SmaI–XhoI sites of pGEX-6P-1 (GE Healthcare), respectively. The GST fusion proteins were expressed in bacteria and purified with Glutathione Sepharose (GE Healthcare).

Histidine-tagged RanQ69L-GTP, importin-β, importin-α, and the ED mutant of importin-α were prepared as described previously (Yokoyama et al., 2008).

Antibodies

Rabbit polyclonal antibodies against *Xenopus* full-length ISWI (1–1046 aa), N-terminal ISWI (1–400 aa), and C-terminal ISWI (746–1046 aa) antibodies were prepared and purified against recombinant proteins according to a standard protocol. A rabbit polyclonal antibody against hSNF2H was purchased from Santa Cruz Biotechnology, Inc.

In vitro MT assays

MT sedimentation assay: recombinant ISWI was incubated with various concentrations of taxol-stabilized MTs at room temperature for 15 min in BRB80 buffer (80 mM K-Pipes, 1 mM $MgCl_2$, and 1 mM EGTA, pH 6.8) or CSF-XB buffer containing 1 mM GTP, 10 µM Taxol, and 0.05 mg/ml BSA. The samples were centrifuged at 100,000 *g* for 10 min at 20°C, and supernatant and pellet were analyzed by SDS-PAGE for Coomassie staining or immunoblot.

MT bundling assay: taxol-stabilized MTs (0.3 µM) incorporating Cy3-labeled tubulin (Hyman et al., 1991) were incubated with recombinant ISWI in BRB80 containing 10 µM taxol at room temperature for 20 min, squashed between slides and coverslips without fixation, and imaged immediately.

MT polymerization assay: recombinant ISWI was incubated at 37°C for 30 min with various concentrations of tubulin purified from pig brains (Castoldi and Popov, 2003) in BRB80 containing 1 mM GTP. The tubulin contained 10% Cy3-labeled tubulin. The samples were fixed with 0.25% glutaraldehyde, 10% glycerol, and 0.1% Triton X-100 in BRB80, and then spun down at 20,000 *g* for 12 min at 20°C onto 12-mm round coverslips through a 25% glycerol cushion in BRB80. The coverslips were post-fixed with cold methanol at −20°C for 10 min, washed with PBS, and mounted on slides.

MT nucleation assay: Talon Dynabeads (10 µl slurry; Invitrogen) were incubated with or without recombinant ISWI (8 µg) at 4°C for 30 min, and washed with PBS containing 0.01% Tween 20. The beads (0.1 µl slurry) were then incubated at 37°C for 30 min in 20 µl of BRB80 containing 20 µM tubulin (2 µM Cy3-tubulin) and 1 mM GTP. The samples were fixed and spun down as described in the MT polymerization assay.

After the assays, images were acquired using a Cellobserver microscope, a Plan-Apochromat 63x NA 1.4 oil objective lens, a Cy3 emission filter, an AxioCam MRm camera, and AxioVision software (all from Carl Zeiss, Inc.).

Electron microscopy

In vitro reactions as described above were spotted onto copper mesh grids, washed with water, and stained with 1.5% uranyl acetate. Images were acquired on an electron microscope (model CM-120; Biotwin).

Immunoprecipitations

Protein A Dynabeads (Invitrogen) were coupled with rabbit IgG or anti–full-length ISWI antibodies following the manufacturer's instructions. Each bead sample (60 µl slurry) was incubated with CSF extracts (100 µl) at 4°C for 90 min, and washed two times with CSF-XB and two times with CSF-XB containing 0.1% Triton X-100. The immunoprecipitates were resolved by SDS-PAGE for Coomassie staining and Western blotting. To examine the MT polymerization activity of the immunoprecipitates, they were incubated at 37°C for 30 min with 20 µM pure tubulin (2 µM Cy3-tubulin) in BRB80 containing 1 mM GTP in the presence or absence of 15 µM RanQ69L, then fixed, and spun onto coverslips.

ATPase assay

The assay was conducted as described previously (Corona et al., 1999).

Immunofluorescence

Xenopus XL177 tissue culture cells were fixed in cold methanol at −20°C for 10 min, and stained with a mixture of full-length ISWI (1–1046 aa),

N-terminal ISWI (1–400 aa), and C-terminal ISWI (746–1046 aa) antibodies (total 3 µg/ml of each 1 µg/ml) followed by Alexa 488–labeled anti–rabbit IgG (Invitrogen). Tubulin was stained with anti–α-tubulin DM 1A (Sigma-Aldrich) followed by Alexa 568–labeled anti–mouse IgG (Invitrogen). DNA was stained with Hoechst 33342. Images were acquired using a Cellobserver microscope, a Plan-Apochromat 63x NA 1.4 oil objective lens, an AxioCam MRm camera, and AxioVision software (all from Carl Zeiss, Inc.).

RanGTP-dependent MT nucleation and stabilization assays in egg extracts

RanGTP-dependent MT nucleation assay: CSF extracts were incubated with 15 µM RanQ69L-GTP and 1 µM Cy3-tubulin at 20°C for 30 min. The samples (Ran spindles and asters) were fixed with 4% formaldehyde and 30% glycerol in BRB80, and spun down at 20,000 *g* for 12 min at 20°C onto 12-mm round coverslips through a 40% glycerol cushion in BRB80. The coverslips were post-fixed with cold methanol at −20°C for 10 min, and mounted on slides directly or immunostained before the mount.

RanGTP-dependent MT stabilization assay: performed as described previously (Yokoyama et al., 2008). In brief, CSF extracts were incubated with 1 µM Cy3-tubulin, 0.15 mg/ml anti-TPX2 antibody, and 2,000 centrosomes/µl in the presence or absence of 15 µM RanQ69L-GTP at 20°C for 30 min. The samples (centrosomal asters) were fixed, spun down, and mounted on slides. The MT length and intensity of centrosomal asters were quantified using a macro written in MatLab.

RNA interference

Drosophila Schneider S2 cells were cultured and RNAi was performed as described previously (Bettencourt-Dias and Goshima, 2009). In brief, dsRNAs against *Drosophila* ISWI (MRC015_H12, HFA07446, and OB2651) were prepared based on the sequence information from the GenomeRNAi database (Horn et al., 2007). Cells (10^6) were incubated with 30 µg dsRNA at 25°C, and analyzed by cell counting and FACS. For immunofluorescence, the part of the cells was attached on coverslips, fixed, and stained with anti–α-tubulin DM 1A and anti–phospho-histone H3 (Millipore) followed by Alexa 568–labeled anti–mouse IgG and Alexa 488–labeled anti–rabbit IgG. DNA was stained with Hoechst 33342. Images were acquired at 0.25-µm z steps using a confocal microscope (model SP5; Leica) equipped with a 63x Plan-Apochromat NA 1.4 oil-immersion objective lens. They were subsequently processed using ImageJ (National Institutes of Health, Bethesda, MD).

Live-cell imaging was performed using S2 cells stably expressing GFP–α-tubulin and CID-mCherry (Coelho et al., 2008) after dsRNA treatment. 4D datasets covering the entire cell volume were collected every 1.5 min with 1-µm z steps at 25°C using a spinning disc confocal microscope (Ultraview Vox; PerkinElmer) equipped with an EC Plan-Neofluar 100x/1.3 oil-immersion objective lens. They were processed using ImageJ.

Online supplemental material

Fig. S1 shows that ISWI binds to MTs with high affinity. Fig. S2 shows that ISWI nucleates MTs in vitro. Fig. S3 shows that the ATPase activity of ISWI is not necessary for MT regulation. Fig. S4 shows that in ISWI-depleted extracts, spindle MTs disappear at anaphase onset and chromosomes do not segregate. Fig. S5 shows that excess ISWI stabilizes RanGTP spindles during anaphase. Video 1 shows a control S2 cell expressing GFP-tubulin and CID-mCherry. Videos 2 and 3 show S2 cells expressing GFP-tubulin and CID-mCherry after dsRNA treatment for ISWI. Online supplemental material is available at http://www.jcb.org/cgi/content/full/jcb.200906020/DC1.

We thank H. Maiato for providing an S2 cell line, A. Perez-Gonzalez for helping FACS analysis, O. Gruss for recombinant active CaMKII, F. Nedelec for writing macros, P. Bieling for the histidine-tagged GFP protein plasmid, K. Crnokic for maintaining frogs, and M. Bettencourt-Dias for advice regarding RNAi experiments. We also thank the Advanced Light Microscopy Facility in EMBL.

H. Yokoyama was supported by the EMBL postdoctoral fellowship.

Submitted: 4 June 2009
Accepted: 17 November 2009

References

Bettencourt-Dias, M., and G. Goshima. 2009. RNAi in *Drosophila* S2 cells as a tool for studying cell cycle progression. *Methods Mol. Biol.* 545:39–62. doi:10.1007/978-1-60327-993-2_3

Brown, E., S. Malakar, and J.E. Krebs. 2007. How many remodelers does it take to make a brain? Diverse and cooperative roles of ATP-dependent chromatin-remodeling complexes in development. *Biochem. Cell Biol.* 85:444–462. doi:10.1139/O07-059

Carazo-Salas, R.E., G. Guarguaglini, O.J. Gruss, A. Segref, E. Karsenti, and I.W. Mattaj. 1999. Generation of GTP-bound Ran by RCC1 is required for chromatin-induced mitotic spindle formation. *Nature.* 400:178–181. doi:10.1038/22133

Carazo-Salas, R.E., O.J. Gruss, I.W. Mattaj, and E. Karsenti. 2001. Ran-GTP coordinates regulation of microtubule nucleation and dynamics during mitotic-spindle assembly. *Nat. Cell Biol.* 3:228–234. doi:10.1038/35060009

Castoldi, M., and A.V. Popov. 2003. Purification of brain tubulin through two cycles of polymerization-depolymerization in a high-molarity buffer. *Protein Expr. Purif.* 32:83–88. doi:10.1016/S1046-5928(03)00218-3

Clarke, P.R., and C. Zhang. 2008. Spatial and temporal coordination of mitosis by Ran GTPase. *Nat. Rev. Mol. Cell Biol.* 9:464–477. doi:10.1038/nrm2410

Coelho, P.A., J. Queiroz-Machado, A.M. Carmo, S. Moutinho-Pereira, H. Maiato, and C.E. Sunkel. 2008. Dual role of topoisomerase II in centromere resolution and aurora B activity. *PLoS Biol.* 6:e207. doi:10.1371/journal.pbio.0060207

Corona, D.F., G. Längst, C.R. Clapier, E.J. Bonte, S. Ferrari, J.W. Tamkun, and P.B. Becker. 1999. ISWI is an ATP-dependent nucleosome remodeling factor. *Mol. Cell.* 3:239–245. doi:10.1016/S1097-2765(00)80314-7

Demeret, C., S. Bocquet, J.M. Lemaítre, P. Françon, and M. Méchali. 2002. Expression of ISWI and its binding to chromatin during the cell cycle and early development. *J. Struct. Biol.* 140:57–66. doi:10.1016/S1047-8477(02)00575-0

Deuring, R., L. Fanti, J.A. Armstrong, M. Sarte, O. Papoulas, M. Prestel, G. Daubresse, M. Verardo, S.L. Moseley, M. Berloco, et al. 2000. The ISWI chromatin-remodeling protein is required for gene expression and the maintenance of higher order chromatin structure in vivo. *Mol. Cell.* 5:355–365. doi:10.1016/S1097-2765(00)80430-X

Dirscherl, S.S., J.J. Henry, and J.E. Krebs. 2005. Neural and eye-specific defects associated with loss of the imitation switch (ISWI) chromatin remodeler in *Xenopus laevis*. *Mech. Dev.* 122:1157–1170. doi:10.1016/j.mod.2005.08.002

Félix, M.A., P. Cohen, and E. Karsenti. 1990. Cdc2 H1 kinase is negatively regulated by a type 2A phosphatase in the *Xenopus* early embryonic cell cycle: evidence from the effects of okadaic acid. *EMBO J.* 9:675–683.

Grüne, T., J. Brzeski, A. Eberharter, C.R. Clapier, D.F. Corona, P.B. Becker, and C.W. Müller. 2003. Crystal structure and functional analysis of a nucleosome recognition module of the remodeling factor ISWI. *Mol. Cell.* 12:449–460. doi:10.1016/S1097-2765(03)00273-9

Gruss, O.J., R.E. Carazo-Salas, C.A. Schatz, G. Guarguaglini, J. Kast, M. Wilm, N. Le Bot, I. Vernos, E. Karsenti, and I.W. Mattaj. 2001. Ran induces spindle assembly by reversing the inhibitory effect of importin alpha on TPX2 activity. *Cell.* 104:83–93. doi:10.1016/S0092-8674(01)00193-3

Hannak, E., and R. Heald. 2006. Investigating mitotic spindle assembly and function in vitro using *Xenopus laevis* egg extracts. *Nat. Protoc.* 1:2305–2314. doi:10.1038/nprot.2006.396

Heald, R., R. Tournebize, T. Blank, R. Sandaltzopoulos, P. Becker, A. Hyman, and E. Karsenti. 1996. Self-organization of microtubules into bipolar spindles around artificial chromosomes in *Xenopus egg* extracts. *Nature.* 382:420–425. doi:10.1038/382420a0

Hetzer, M., O.J. Gruss, and I.W. Mattaj. 2002. The Ran GTPase as a marker of chromosome position in spindle formation and nuclear envelope assembly. *Nat. Cell Biol.* 4:E177–E184. doi:10.1038/ncb0702-e177

Horn, T., Z. Arziman, J. Berger, and M. Boutros. 2007. GenomeRNAi: a database for cell-based RNAi phenotypes. *Nucleic Acids Res.* 35(Database issue):D492–D497. doi:10.1093/nar/gkl906

Hsu, J.M., Y.C. Lee, C.T. Yu, and C.Y. Huang. 2004. Fbx7 functions in the SCF complex regulating Cdk1-cyclin B-phosphorylated hepatoma up-regulated protein (HURP) proteolysis by a proline-rich region. *J. Biol. Chem.* 279:32592–32602. doi:10.1074/jbc.M404950200

Hyman, A., D. Drechsel, D. Kellogg, S. Salser, K. Sawin, P. Steffen, L. Wordeman, and T. Mitchison. 1991. Preparation of modified tubulins. *Methods Enzymol.* 196:478–485. doi:10.1016/0076-6879(91)96041-O

Kalab, P., and R. Heald. 2008. The RanGTP gradient—a GPS for the mitotic spindle. *J. Cell Sci.* 121:1577–1586. doi:10.1242/jcs.005959

Lazzaro, M.A., and D.J. Picketts. 2001. Cloning and characterization of the murine Imitation Switch (ISWI) genes: differential expression patterns suggest distinct developmental roles for Snf2h and Snf2l. *J. Neurochem.* 77:1145–1156. doi:10.1046/j.1471-4159.2001.00324.x

Liska, A.J., A.V. Popov, S. Sunyaev, P. Coughlin, B. Habermann, A. Shevchenko, P. Bork, E. Karsenti, and A. Shevchenko. 2004. Homology-based functional proteomics by mass spectrometry: application to the *Xenopus* microtubule-associated proteome. *Proteomics.* 4:2707–2721. doi:10.1002/pmic.200300813

MacCallum, D.E., A. Losada, R. Kobayashi, and T. Hirano. 2002. ISWI remodeling complexes in *Xenopus* egg extracts: identification as major chromosomal components that are regulated by INCENP-aurora B. *Mol. Biol. Cell.* 13:25–39. doi:10.1091/mbc.01-09-0441

Maresca, T.J., H. Niederstrasser, K. Weis, and R. Heald. 2005. Xnf7 contributes to spindle integrity through its microtubule-bundling activity. *Curr. Biol.* 15:1755–1761. doi:10.1016/j.cub.2005.08.049

Matos, I., A.J. Pereira, M. Lince-Faria, L.A. Cameron, E.D. Salmon, and H. Maiato. 2009. Synchronizing chromosome segregation by flux-dependent force equalization at kinetochores. *J. Cell Biol.* 186:11–26. doi:10.1083/jcb.200904153

Murray, A. 1991. Cell cycle extracts. *In Xenopus laevis*: Practical uses in cell and molecular biology. Vol. 36. B.K. Kay and H.B. Peng, editors. Academic Press, Inc. San Diego. 581–605.

Reber, S., S. Over, I. Kronja, and O.J. Gruss. 2008. CaM kinase II initiates meiotic spindle depolymerization independently of APC/C activation. *J. Cell Biol.* 183:1007–1017. doi:10.1083/jcb.200807006

Stewart, S., and G. Fang. 2005. Anaphase-promoting complex/cyclosome controls the stability of TPX2 during mitotic exit. *Mol. Cell. Biol.* 25:10516–10527. doi:10.1128/MCB.25.23.10516-10527.2005

Stopka, T., and A.I. Skoultchi. 2003. The ISWI ATPase Snf2h is required for early mouse development. *Proc. Natl. Acad. Sci. USA.* 100:14097–14102. doi:10.1073/pnas.2336105100

Trachtulcová, P., I. Janatová, S.D. Kohlwein, and J. Hasek. 2000. *Saccharomyces cerevisiae* gene ISW2 encodes a microtubule-interacting protein required for premeiotic DNA replication. *Yeast.* 16:35–47. doi:10.1002/(SICI)1097-0061(20000115)16:1<35::AID-YEA504>3.0.CO;2-0

Watson, J.V., S.H. Chambers, and P.J. Smith. 1987. A pragmatic approach to the analysis of DNA histograms with a definable G1 peak. *Cytometry.* 8:1–8. doi:10.1002/cyto.990080101

Yokoyama, H., O.J. Gruss, S. Rybina, M. Caudron, M. Schelder, M. Wilm, I.W. Mattaj, and E. Karsenti. 2008. Cdk11 is a RanGTP-dependent microtubule stabilization factor that regulates spindle assembly rate. *J. Cell Biol.* 180:867–875. doi:10.1083/jcb.200706189